Macromolecules
ARTICLE

Macromolecules **2009**, *42*, 4661–4666 **4661**
DOI: 10.1021/ma9005445

Influence of Molecular Weight Distribution on the Gelation of P3HT and Its Impact on the Photovoltaic Performance

Markus Koppe*,† and Christoph J. Brabec†,‡

†*Konarka Technologies GmbH, Altenbergerstrasse 69, A-4040 Linz, Austria, and* ‡*Konarka Technologies GmbH, Landgrabenstrasse 94, D-90443 Nürnberg, Germany*

Sabrina Heiml and Alois Schausberger

Johannes Kepler University, Polymer Science, Altenbergerstr. 69, A-4040 Linz, Austria

Warren Duffy

Merck Chemicals, Chilworth Science Park, Southampton, U.K.

Martin Heeney and Iain McCulloch

Imperial College London, London SW7 2AZ, U.K.

Received March 13, 2009; Revised Manuscript Received May 8, 2009

ABSTRACT: P3HT is a semirigid and semicrystalline polymer with a strong tendency to postcrystallize in solid films upon thermal annealing. Recent investigations showed that macroscopic, crystalline P3HT fibers can already be precipitated from solution, depending on the combination of solvent systems used. In this paper we investigate the mechanism and the dynamics of gelation in P3HT solutions. Rheological and absorption measurements in solution reveal a distinct two-step mechanism. In a first step, aggregates are formed which, in a second step, link to each other into a thermoreversible gel. The correlation between the gelation dynamics and the molecular weight distribution is discussed in more detail for a nonhazardous, printing friendly solvent system.

1. Introduction

As the need for renewable energy sources becomes more and more urgent, photovoltaic energy conversion is attracting increasing interest. Because of the worldwide concentrated and concerted R&D efforts, the power conversion efficiency of organic solar cells (OSC, i.e., solar cells based on solution processable blends of conjugated polymers with fullerenes) recently exceeded the 5% limit[1] for 1 cm^2 cells and hit the 6% level for small area solar cells.[2,3] These efficiencies are significantly smaller than those reported for inorganic solar cells but nevertheless demonstrate in an impressive way that solution processing of solar cells will become a viable technology platform in the near future. Specifically, the efficiency of organic solar cells based on poly(3-hexylthiophene) (P3HT) blended with fullerenes has continuously improved over the past couple of years.[4−6]

Solar cells based on a bulk heterojunction[7] of regioregular P3HT and [6,6]-phenyl-C_{61}-butyric acid methyl ester (PCBM) have been reported among the highest performing material systems to date. Beside improvements on the device side like thermal[8] or solvent annealing procedures,[9,10] use of selective solvents,[11,12] and solvent mixtures,[13,14] an essential part came from continuous improvements in the material itself, i.e., reduction of synthetic impurities, higher regioregularities,[15,16] and increased molecular weight.[17−20] It is worthwhile to note that much of the improvement in device performance resulted from the increased crystallinity and charge carrier mobilities of the P3HT and fullerene phases which reduced charge carrier recombination losses.[15,21−23]

As previously mentioned, one of the main attractions of organic solar cells[24] is that industrial mass production can potentially occur via solution-based roll-to-roll printing and coating. Printing and coating is a production process with low energy consumption and a positive life cycle balance impact, subject to using environmentally compatible solvent systems. Halogenated solvents are generally environmentally harmful and should be avoided per se. Expensive and energy-consuming solvent recovery precautions are required in case the limited solubility of the active components requires halogenated solvent systems like chlorobenzene (CB) or *o*-dichlorobenzene (*o*-DCB). The working horses among the printing and environmentally friendly solvents are systems based on toluene or isomers of xylene. Xylenes have a better solubility for organic semiconductors than toluene and are usually preferred. Besides, toluene was shown earlier to give an unfavorable morphology for specific material systems.[11] For all these reasons, we concentrated our investigation in this study on *o*-xylene, which offers a good compromise between performance and being nonhazardous. However, a drawback of printing P3HT with a certain molecular weight distribution out of *o*-xylene is the rather fast formation of gels, causing particles and film defects and giving rise to a reduction of the solution's shelf lifetime. Several investigations have reported that *o*-xylene (or similar solvents) triggers gelation in rodlike polymers rather quickly.[25−27] In this work we

*Corresponding author: E-mail: mkoppe@konarka.com; Fax: +43732 2468 5119.

© 2009 American Chemical Society
Published on Web 06/05/2009

investigate the mechanism responsible for the gelation of P3HT in *o*-xylene and outline a set of polymer specifications that allow the control of gelation. In detail, we report on P3HT polymers with a number-average molecular weight (M_w) between 26 200 and 153 000 g mol^{-1} and investigate how the molecular weight distribution controls the degree of aggregation, gelation kinetics, and the resulting photovoltaic performance.

2. Experimental Section

The investigated regioregular P3HT batches were M_w/M_n = 26 200/13 000 g mol^{-1} (polydispersity (PD) = 2.02), RR = 95%; M_w/M_n = 72 800/34 400 g mol^{-1} (PD = 2.12), RR = 98.5%; M_w/M_n = 153 800/62 500 g mol^{-1} (PD = 2.46), RR = 98.5%. These batches are subsequently called low (L-M_w), average (A-M_w), and high (H-M_w) molecular weight. Molecular weight determinations were carried out in chlorobenzene solution at 60 °C on an Agilent 1100 series HPLC using two Polymer Laboratories mixed B columns in series, and the system was calibrated against narrow weight PL polystyrene calibration standards. Blend solutions of the low and the high molecular weight polymers were investigated to understand the influence of polydispersity (PD).

Photovoltaic devices were fabricated by doctor balding[28] the semiconductor solution on indium tin oxide (ITO) covered glass substrates (Merck) substrates, which were covered with a 100 nm layer of poly(3,4-ethylenedioxythiophene)/poly(styrenesulfonic acid) (PEDOT:PSS) (Baytron PH from H.C. Starck). Photovoltaic layers, consisting of the various P3HT batches and mixtures thereof (provided by Merck Ltd.), were blended with the methanofullerene PCBM ([6,6]-phenyl-C_{61}-butyric acid methyl ester) in 1:1 weight ratios and dissolved with 1 wt % in *o*-xylene. The typical dry film thickness was around 170 nm as determined by atomic force microscopy (AFM) measurements and comparable for all devices shown herein. The LiF/Al (0.6 nm/80 nm) metal electrode was thermally evaporated. The current−voltage characteristics were measured using a Keithley 2400 SMU. Illumination was provided by AM1.5G irradiation from an Oriel xenon solar simulator (100 mW cm^{-2}) with a spectral mismatch of ~95% for P3HT devices.

Atomic force microscope measurements were carried out with a Nanosurf Easyscan 2 in contact mode.

Viscosity measurements were carried out with a Paar Physica rotational rheometer equipped with a temperature-controlled cylinder. For all presented measurements, a 80 °C hot 1 wt % *o*-xylene solution was fed into the cylinder rheometer with both cylinders tempered at 25 °C and measured under constant angular shear frequency (ω = 1 s^{-1}).

Total reflection measurements were carried out with a Hellma UV−vis−ATR sensor coupled via SMA plugs to an Ocean Optics fiber spectrophotometer on 1 wt % *o*-xylene solutions. The temperature of the solutions was controlled within ±0.2 °C by a heated stirrer. The stirring speed was kept constant for all measurements to avoid changes in shear forces.

3. Results and Discussion

3.1. Rheological Investigations of P3HT Solutions in *o*-Xylene. A fluid is defined as a Newtonian liquid when its viscosity remains constant under various shear rates. Highly diluted polymer solutions typically behave as Newtonian solutions, indicating that the individual polymer coils do not interact with each other. Figure 1 shows that this is true for P3HT solutions within the concentration regime used for investigations in this work. Further, the viscosity of the low and average molecular weight P3HT solutions in *o*-xylene were found to only weakly depend on the polymer concentration in the regime between 0.1 and 1 wt %.[29] This allows us to treat freshly prepared, well-dissolved P3HT solutions of moderate molecular weight as a Newtonian liquid, where the single polymer chains do not interact with each other. The steep ascending part of the curves shown in Figure 1 is attributed to artifacts caused by the viscosimeter.

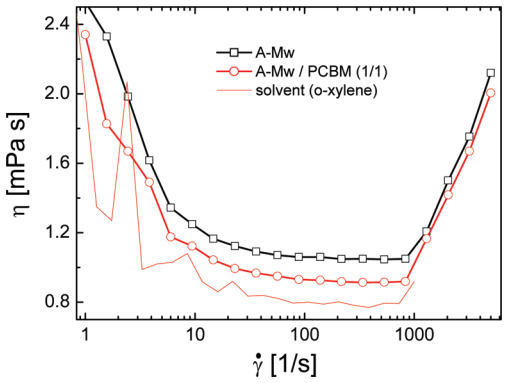

Figure 1. Shear rate vs viscosity relations of a pristine A-M_w (M_w = 72 800 g mol^{-1}) *o*-xylene solution (open squares) and a fullerene blended (open circles) A-M_w (M_w = 72 800 g mol^{-1}) *o*-xylene solution. Concentrations of investigated *o*-xylene solutions are all 1 wt %. The full line indicates the pure solvent.

On the other hand, gels frequently show thixotropic flow behavior, where the viscosity is lowered under increased shear. As the shear stress is increased, more and more entanglements between the polymer chains are becoming disentangled, and the viscosity gets reduced.

Transient viscosity measurements are a useful tool to investigate the interaction of polymer coils in solution. A strong viscosity increase of the solution is typical of chemical or physical cross-linking between the polymer chains. Such a viscosity increase is indicative that the polymer coils do interact with each other, as expected for semidilute or concentrated systems. There, the relative viscosity progression reflects the degree of gelation while the absolute value of the viscosity reflects the density of entanglement points within the gel.

The temporal evolution of the storage moduli G' and loss moduli G'' are recorded at a constant angular shear frequency (ω = 1 s^{-1}). The complex viscosity η^* (2), as calculated from the complex moduli G^* (1), is plotted as a function of time to visualize the onset of gelation as discussed in the following section.

$$|G^*| = \sqrt{G' + G''} \tag{1}$$

$$|\eta^*| = \frac{|G^*|}{\omega} \tag{2}$$

Figure 2 shows a semilog plot of the absolute value of the complex viscosity η^* vs time for several different polymer batches. A strong increase in viscosity by several orders in magnitude is observed over time for nearly all investigated systems and is tentatively assigned to the formation of a gel. The viscosity rise can occur on very rapid time scales. The solution of average molecular weight P3HT (A-M_w; M_w = 72 800 g mol^{-1}) polymer only took a few minutes before being completely gelled, while the solutions mixed with the low molecular weight L-M_w batch took several hours before gelling even started. For the pristine low molecular weight fraction L-M_w (M_w = 26 200 g mol^{-1}) no gelation was observed at all.

In all cases we found the gelation to be completely reversible. Heating up the gel dissolved it completely and resulted in the restoration of a Newtonian solution, as expected for rodlike polymers forming a thermoreversible network by physical linking of the polymer chains.

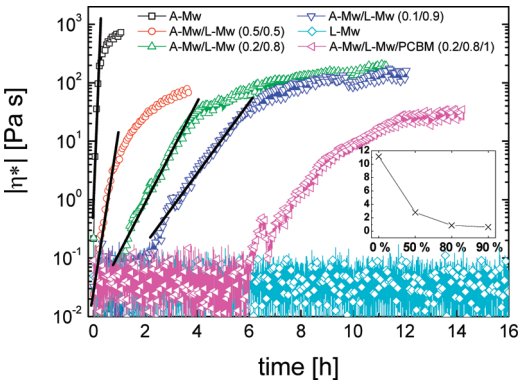

Figure 2. Rotational rheometer viscosity measurements of various M_w compositions at 25 °C dissolved in *o*-xylene (1 wt %). A-M_w (M_w = 72 800 g mol^{-1}), L-M_w (M_w = 26 200 g mol^{-1}). Full lines are linear fits to the viscosity progression. The inset shows the slopes of the linear fits over M_w with increasing contents of L-M_w mixed into A-M_w (0, 50, 80, and 90 wt %).

As shown in Figure 2, we observe that the molecular weight is the driving force behind the gelation dynamics. We further observed that the higher the molecular weight the higher also is the viscosity, i.e., the density of entanglement points between the polymer chains. The P3HT with average molecular weight A-M_w gels within few minutes, and only the addition of significant amounts (50−90 wt %) of the low molecular weight fraction L-M_w allows the delay of the onset of gelation by up to 2 h. Linear fits to the viscosity in the early gelling regime were used to determine the gelation rates $d_{gelation}/dt$. These slopes are plotted in the inset of Figure 2 and visualize the trend that lower molecular weights lead not only to longer gelation delays but also to slower gelation rates. The low molecular weight fraction L-M_w does not gel at all within the observation period of time (24 h), while the gelation of the high molecular weight batch H-M_w was too fast to record.

3.2. Optical Measurements: Attenuated Total Reflection in Solution. P3HT is well-known to form aggregates in solution.[30] These aggregates are induced by $\pi-\pi$ interaction of the thiophene rings and can be monitored by solution absorption measurements. The absorption of amorphous P3HT peaks takes place at around 470 nm while the aggregated P3HT chains give rise to more narrow absorption features. These features, and their harmonic progressions, are found in the 530−610 nm regime. Attenuated total reflection (ATR) absorption measurements were chosen to monitor the onset of aggregation. Standard transmission measurement cuvettes were unsuitable to record absorption over time due to the high optical density of a 1 wt % solution. ATR spectroscopy further allows continuous stirring of the solution, which is a necessary technical detail to guarantee comparable and reproducible conditions. Only normalized ATR spectra are reported in the following section. The degree of aggregation is evaluated and discussed at the hands of the height of the absorption peak at ~610 nm.

Figures 3a,b,d show the optical spectra reflecting the degree of aggregation for high, average, and low molecular weight P3HT. In addition, Figure 3c shows the data for a (0.8/0.2) mixture of the low molecular weight L-M_w with the average molecular weight A-M_w P3HT batch. All polymer fractions were investigated as pristine solutions as well as blended with PCBM in a 1/1 (w/w) ratio.

A clear trend between the degree of aggregation and the molecular weight is observed. The higher the molecular weight of the polymer, the stronger is the aggregation. The high molecular weight batch shows a significant degree of aggregation even at temperatures as high as 65 °C (Figure 3a) whereas all other batches/mixtures are still completely amorphous at such high solution temperatures. In all cases, addition of PCBM, what acts as a diluting agent, lowers the degree of P3HT aggregation. Taking into account that the P3HT/PCBM solutions have an higher absolute solid state content compared to pristine P3HT solutions, and assuming that PCBM does not solubilize P3HT, we explain the lower aggregation of P3HT/PCBM solutions by an incorporation of PCBM into the polymer matrix.

To better distinguish between the formation of aggregates as seen in the ATR spectra and the formation of physical gels as seen from the viscosity measurements, transient ATR spectra were recorded.

Figure 4 shows the normalized aggregation rate over time at room temperature. Not surprisingly, the average molecular weight A-M_w P3HT solution aggregates most rapidly. Within a few minutes the aggregation process is finished, and the signal saturates. The time until aggregation becomes saturated can be delayed by up to 2 h upon addition of large amounts (80−90 wt %) of low molecular weight fraction. We determined the aggregation time as the peak value of the first derivative of the aggregation rate curves, as shown in the inset of Figure 4. Figure 4 clearly shows that the molecular weight is determining not only the aggregation intensity but also the aggregation kinetics.

3.3. Schematic Process of Gelation. Figures 2 and 4 suggest that aggregation and gelation follow a different kinetic behavior. The circles in Figure 4 indicate the starting point of gelation as determined by the solution viscosity measurements. This observation can be interpreted in the following way: Formation of solution aggregates occurs over a very fast time scale. Depending on the molecular weight, individual polymer chains begin to aggregate. Aggregation continues until the maximum number of $\pi-\pi$ interactions are formed within a single chain. Aggregation within a single chain mainly modifies the free volume of the chain, and little change in viscosity is expected at this stage. At a time when aggregation begins to saturate, viscosity starts to increase. At this point in time, single but highly aggregated chains begin to interact and physically cross-link with each other. Figure 5 visualizes the scheme of gelation: when aggregation starts, the solution turns from yellow-orange to dark red (L-M_w) or dark violet (A-M_w and H-M_w) but apparently does not change viscosity. After aggregation is complete and starts to saturate, gelation kicks in and starts to form a physical network. A two-step process can be concluded: phase 1 consists of the coil to rod formation leading to aggregation while in phase 2 these ordered domains can physically link to each other. Both phases have been studied for several rodlike macromolecules and are still under investigation.[25−27,29,31] P3HT, dissolved in *o*-xylene, follows this scheme.

3.4. Device Performance. Solar cells were produced from the various P3HT fractions. All devices presented in this paper were processed with identical blading and annealing parameters. The correlation between the solar cell performance and the molecular weight of the P3HT batch is summarized in Figure 6. Figure 6a summarizes the *jV* curves for the various M_w batches, while Figure 6b presents the power efficiency of the devices as measured under AM1.5 conditions. The power efficiency is the product of the short-circuit current (J_{sc}), the open-circuit voltage (V_{oc}), and the fill factor (FF) divided by the incident light power I_{light}.

$$\eta = J_{sc} V_{oc} FF / I_{light} \quad (3)$$

The main difference in efficiency arises from the short-circuit current, while V_{oc} and FF turn out to be quite insensitive to

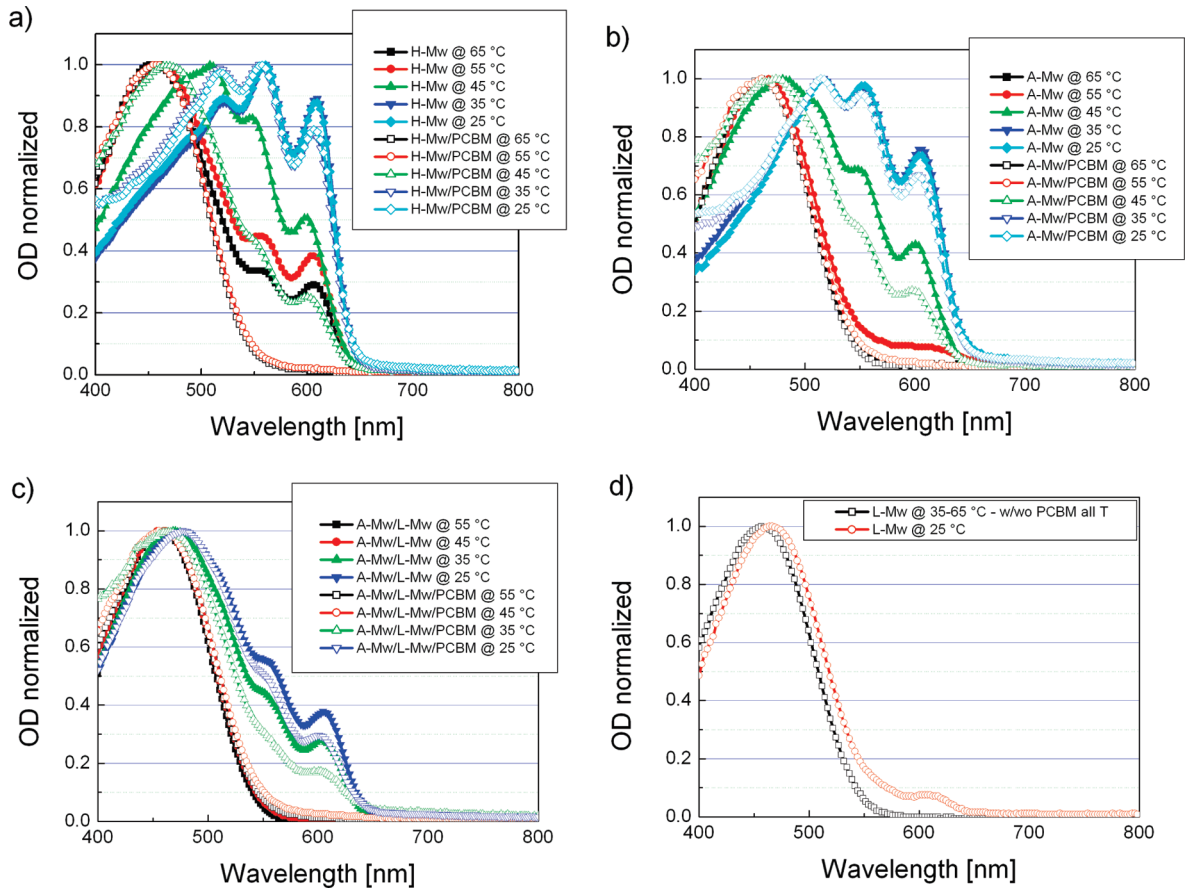

Figure 3. Temperature dependence of the polymer aggregation for (a) H-M_w (M_w = 153 800 g mol^{-1}) (b) A-M_w (M_w = 72 800 g mol^{-1}), and (c) mixture A-M_w/L-M_w (0.2/0.8). Open symbols indicate solutions with PCBM while closed symbols indicate solutions without PCBM. (d) Shows representative data for the whole series of L-M_w (M_w = 26 200 g mol^{-1}).

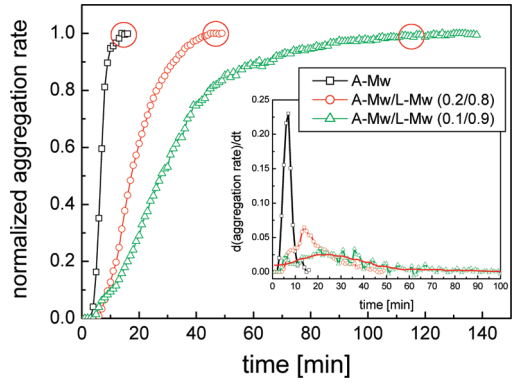

Figure 4. Normalized aggregation rates vs time for three different polymer solutions. The circles indicate the onset of viscosity increase as observed in Figure 2. The inset shows the first derivative of the aggregation rates for the three polymer solutions. A-M_w (M_w = 72 800 g mol^{-1}), L-M_w (M_w = 26 200 g mol^{-1}).

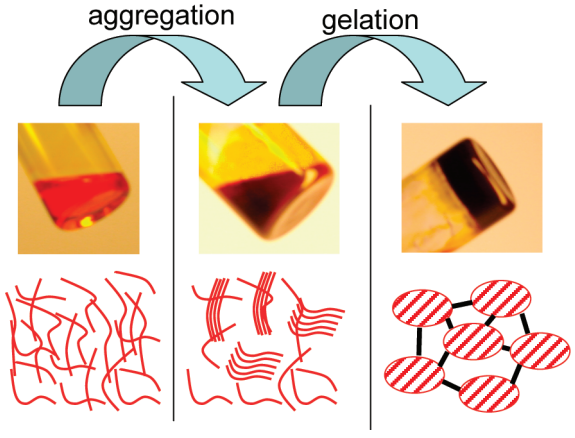

Figure 5. Photos and schematic demonstration of the discussed two-step gelation process of a 1 wt % *o*-xylene−P3HT solution of A-M_w batch (M_w = 72 800 g mol^{-1}).

the molecular weight variations, with the exception of the high molecular weight batch H-M_w, where the lower short-circuit current is accompanied by a slightly lower fill factor. Note that the H-M_w batch cells were quite insensitive to the normal annealing procedures. Additional annealing steps at higher temperatures and/or with longer annealing times were applied but also did not result in higher performance. These observations go hand in hand with what was reported for P3HT processed from chlorobenzene earlier.[17−19,32]

Adding 80 wt % of the low molecular weight fraction L-M_w to higher molecular weight fractions A-M_w and H-M_w allows a modification of the performance. The performance of the average molecular weight fraction A-M_w (M_w = 72 800 g mol^{-1}) gets slightly reduced upon addition of the low molecular weight fraction L-M_w, while addition of 80 wt % of the L-M_w fraction to the high molecular weight batch H-M_w significantly increased the performance. In summary, an average molecular weight of 40 000−50 000 g mol^{-1} appears to be a good compromise between high performance and reduced gelation for P3HT when processed out of *o*-xylene. And indeed, high efficiency in parallel to reduced gelation was observed for a batch with a M_w = 43 700 g mol^{-1}. The PD index plays only a minor role in the photovoltaic performance.

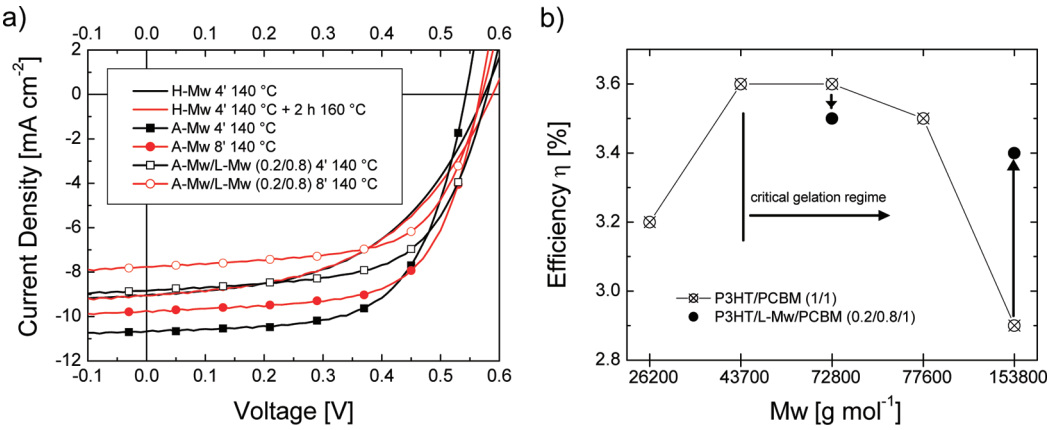

Figure 6. (a) *jV* data of temperature-annealed P3HT/PCBM (1/1) solar cells for various molecular weights. H-M_w (M_w = 153 800 g mol^{-1}) (full line), A-M_w (M_w = 72 800 g mol^{-1}) (full symbols), and a A-M_w/L-M_w (0.2/0.8) blend (open symbols) before and after and additional annealing step. (b) Photovoltaic performance vs molecular weight M_w [g mol^{-1}]. Crossed open symbols indicate the performance of the particular polymer blended with PCBM. Closed symbols indicate the performance after particular blending with 80 wt % of low molecular weight fraction L-M_w (M_w = 26 200 g mol^{-1}).

3.5. Surface Topography via AFM. The topography and the device surface of individual P3HT films with different molecular weight distributions were investigated by AFM. The highest surface roughness was found for the highest molecular weight batches. The highest molecular weight batch (153 800 g mol^{-1}) resulted in the roughest films (40−60 nm). Reducing the concentration of the high molecular weight fraction did smooth the surface of the devices significantly, resulting in a roughness < 5 nm (H-M_w/L-M_w (0.1/0.9)). The significant roughness of the H-M_w containing film could indicate the presence of big polymer aggregates and may play a role in the reduced OPV device performance (Figure 6).

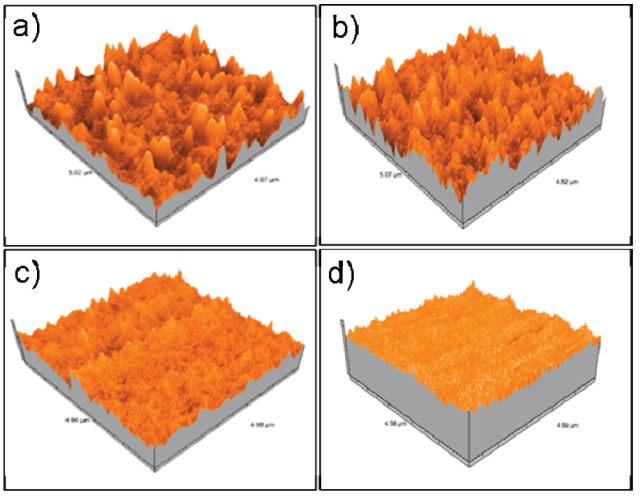

Figure 7. AFM surface scans (5 μm × 5 μm) of (a) P3HT H-M_w (M_w = 153 800 g mol^{-1}), (b) H-M_w/L-M_w (0.75/0.25), (c) H-M_w/L-M_w (0.5/0.5), and (d) H-M_w/L-M_w (0.1/0.9); L-M_w (M_w = 26 200 g mol^{-1}). All layers were processed out of a 1 wt % *o*-xylene solution at 60 °C.

4. Discussion and Summary

The correlation between molecular weight and P3HT conformation has been investigated to rather wide detail in the past. Brinkmann et al.[33] reported that the crystallinity decreases with increasing molecular weight. In good agreement with this, Schilinsky et al.[19] reported on a lower threshold for the molecular weight of P3HT to give sufficient device performance. Transport studies suggest that highest molecular weight P3HT also should give highest mobility.[21] To determine the optimum molecular weight for solar cell applications, poly(3-hexylthiophene)s with a wide range of molecular weights from a few thousand up to 300 000 were screened,[32] and a mix of high molecular weight with low molecular weight fractions was suggested as a necessary material parameter for optimized performance.[17]

This investigation was focused on a rather unusual solvent system for P3HT/PCBM solar cells. Despite the lower solubility of *o*-xylene compared to the standard solvent systems like chlorobenzene or *o*-dichlorobenzene, our findings confirm the general correlation between molecular weight and solar cell performance. In addition, our investigations bring a new rational behind the observed molecular weight performance correlations, which is based on the ability to control gelation.

Gelation is a serious processing problem for electronic inks. It shortens the lifetime of the ink, causes particle problems, and can influence the morphology and performance of the printed film. P3HT, dissolved in *o*-xylene, shows a strong tendency to gel depending on its molecular weight. The gelation appears to run in a two-step process. In the first step, single, isolated polymer chains start to form $\pi-\pi$ aggregates, which can be observed as specific absorption features in the solution. In the second phase, the individual aggregated chains begin to link to each other and form a gel. The formation of the gel and especially the starting point of the gelling can be identified by an increase in viscosity.

The kinetics and the intensity of these phenomena strongly depend on the material specifications of the P3HT, namely on its molecular weight and its regioregularity. The higher the molecular weight of P3HT, the faster and stronger aggregation and gelation do occur. Aggregation and gelation can develop in temporal subsequent steps. The formation of a gel typically starts after aggregation has saturated. Addition of "dilutants" can delay and even completely suppress the aggregation and gelation of higher molecular weight P3HT. PCBM as well as low molecular weight P3HT can act as such dilutants.

Aggregation of P3HT is an essential process to guarantee high solar cell performance. Well-aggregated P3HT/PCBM solar cells show a non-Langevin recombination kinetics, which is a key parameter for high performance. The thermomechanical properties of a P3HT with a molecular weight of more than 150 000 g mol^{-1} restrict the reorientation of the polymer/fullerene network during annealing and lead to lower device performance.

Concluding, the material specs for P3HT solar cells actually are quite narrow. We have focused this discussion on the impact of the molecular weight on aggregation, gelation, and device performance, but it has to be taken into account that regioregularity will play a major role in these processes as well.[16]

A well-chosen balance between molecular weight and regioregularity is essential for a good compromise between high solar cell performance and processability.

Acknowledgment. We acknowledge public funding from the EC project Olatronics (FP7-216211-OLATRONICS) and the BMBF project EOS (EMOP03151308). Jürgen Parisi (University Oldenburg) is acknowledged for helpful discussions.

References and Notes

(1) Green, M. A.; Emery, K.; Hishikawa, Y.; Warta, W. *Prog. Photovoltaics* **2008**, *16*, 435–440.
(2) Plastic eletronics conference, **2008**, Berlin, Plextronics announcment.
(3) Konarka (www.konarka.com) press release from the 15.12.2008.
(4) Ma, W.; Yang, C.; Gong, X.; Lee, K.; Heeger, A. J. *Adv. Funct. Mater.* **2005**, *15*, 1617–1622.
(5) Li, G.; Shrotriya, V.; Yao, Y.; Yang, Y. *J. Appl. Phys.* **2005**, *98*, 43704–43704/5.
(6) Schilinsky, P.; Waldauf, C.; Brabec, C. J. *Adv. Funct. Mater.* **2006**, *16*, 1669–1672.
(7) Yu, G.; Gao, J.; Hummelen, J. C.; Wudl, F.; Heeger, A. J. *Science* **1995**, *270*, 1789–1791.
(8) Padinger, F.; Rittberger, R. S.; Sariciftci, N. S. *Adv. Funct. Mater.* **2003**, *13*, 85–88.
(9) Li, G.; Yao, Y.; Yang, H.; Shrotriya, V.; Yang, G.; Yang, Y. *Adv. Funct. Mater.* **2007**, *17*, 1636–1644.
(10) Zhao, Y.; Xie, Z.; Qu, Y.; Geng, Y.; Wang, L. *Appl. Phys. Lett.* **2007**, *91*, 43504–43508.
(11) Shaheen, S. E.; Brabec, C. J.; Serdar Sariciftci, N.; Padinger, F.; Fromherz, T.; Hummelen, J. C. *Appl. Phys. Lett.* **2001**, *78*, 841–843.
(12) Chang, J.; Sun, B.; Breiby, D. W.; Nielsen, M. M.; Solling, T. I.; Giles, M.; McCulloch, I.; Sirringhaus, H. *Chem. Mater.* **2004**, *16*, 4772–4776.
(13) Moulé, A. J.; Meerholz, K. *Adv. Mater.* **2008**, *20*, 240–245.
(14) Yao, Y.; Hou, J.; Xu, Z.; Li, G.; Yang, Y. *Adv. Funct. Mater.* **2008**, *18*, 1783–1789.
(15) Sirringhaus, H.; Brown, P. J.; Friend, R. H.; Nielsen, M. M.; Bechgaard, K.; Langeveld-Voss, B. M. W.; Spiering, A. J. H.; Janssen, R. A. J.; Meijer, E. W.; Herwig, P.; de Leeuw, D. M. *Nature (London)* **1999**, *401*, 685–688.
(16) Kim, Y.; Cook, S.; Tuladhar, S. M.; Choulis, S. A.; Nelson, J.; Durrant, J. R.; Bradley, D. C.; Giles, M.; McCulloch, I.; Ha, C.-S.; Ree, M. *Nat. Mater.* **2006**, *5*, 197–203.
(17) Ma, W.; Kim, J. Y.; Lee, K.; Heeger, A. J. *Macromol. Rapid Commun.* **2007**, *28*, 1776–1780.
(18) Hiorns, R. C.; de Bettignies, R.; Leroy, J.; Bailly, S.; Firon, M.; Sentein, C.; Khoukh, A.; Preud'homme, H.; Dagron-Lartigau, C. *Adv. Funct. Mater.* **2006**, *16*, 2263–2273.
(19) Schilinsky, P.; Asawapirom, U.; Scherf, U.; Biele, M.; Brabec, C. J. *Chem. Mater.* **2005**, *17*, 2175–2180.
(20) Ballantyne, A. M.; Chen, L.; Dane, J.; Hammant, T.; Braun, F. M.; Heeney, M.; Duffy, W.; McCulloch, I.; Bradley, D. D. C.; Nelson, J. *Adv. Funct. Mater.* **2008**, *18*, 2373–2380.
(21) Zen, A.; Pflaum, J.; Hirschmann, S.; Zhuang, W.; Jaiser, F.; Asawapirom, U.; Rabe, J. P.; Scherf, U.; Neher, D. *Adv. Funct. Mater.* **2004**, *14*−*8*, 757–764.
(22) Kline, R. J.; McGehee, M. D.; Kadnikova, E. N.; Liu, J.; Fréchet, J. M. J. *Adv. Mater.* **2003**, *15*−*18*, 1519–1522.
(23) Goh, C.; Kline, R. J.; McGehee, M. D.; Kadnikova, E. N.; Fréchet, J. M. J. *Appl. Phys. Lett.* **2005**, *86*, 122110–122110/3.
(24) Yu, G.; Gao, J.; Hummelen, J. C.; Wudl, F.; Heeger, A. J. *Science* **1995**, *270*, 1789–1791.
(25) Tipton, D. L.; Russo, P. S. *Macromolecules* **1996**, *29*, 7402–7411.
(26) Olsen, B. D.; Segalman, R. A. *Mater. Sci. Eng., R* **2008**, *62*, 37–66.
(27) Malik, S.; Nandi, A. K. *J. Appl. Polym. Sci.* **2007**, *103*, 2528–2537.
(28) Pestotnik, D. Diploma Thesis at the Hogeschool van Utrecht, The Netherlands, 2002.
(29) Heiml, S. Master Thesis, Johannes Kepler University Linz, **2006.**
(30) Yamamoto, T.; Komarudin, D.; Arai, M.; Lee, B.-L.; Suganuma, H.; Asakawa, N.; Inoue, Y.; Kubota, K.; Sasaki, S.; Fukuda, T.; Matsuda, H. *J. Am. Chem. Soc.* **2008**, *120*, 2047–2058.
(31) Sinclair, M.; Lim, K. C.; Heeger, A. J. *Phys. Rev. Lett.* **1983**, *51*, 1768–1771.
(32) Hiorns, R. C.; de Bettignies, R.; Leroy, J.; Bailly, S.; Firon, M.; Sentein, C.; Preud'homme, H.; Dagron-Lartigau, C. *Eur. Phys. J. Appl. Phys.* **2006**, *36*, 295–300.
(33) Brinkmann, M.; Rannou, P. *Adv. Funct. Mater.* **2007**, *17*, 101–108.